JGR Space Physics

RESEARCH ARTICLE
10.1029/2024JA033105

Special Collection:
Dynamical processes in space plasmas

Electron Dissipation and Electromagnetic Work

Yan Yang (杨艳)[1], Subash Adhikari[1], and William H. Matthaeus[1]

[1]Department of Physics and Astronomy, University of Delaware, Newark, DE, USA

Abstract With the increase in technical capabilities of computer simulation in recent years, it has become feasible to quantify the degradation of fluid scale plasma and electromagnetic energies in favor of increases of internal energies. While it is understood that electromagnetic energy can be exchanged with fluid scale velocities, it is the pressure strain interaction that exchanges energy between fluid motions and internal energy. Here using simulations of both turbulence and reconnection we show that for electrons, the pressure strain and electromagnetic work are closely related and are frequently comparable when appropriate time and spatial averaging is applied. Otherwise, the instantaneous spatial averaged pressure strain and electromagnetic work are nearly equal for slowly evolving systems, like the reconnection case, while they differ significantly in rapidly evolving systems, like the turbulence case. This clarifies the relationship between these two quantities, which are each frequently used as measures of dissipation.

Plain Language Summary The electromagnetic field changes the fluid velocity of each type of plasma particle. Meanwhile, the pressure of each plasma species, interacts with nonuniform fluid velocities to produce heat. The intermediate steps are in general, complicated, but because electrons are so light, a special simplifying approximation holds, equating properly averaged electromagnetic work on electrons to the rate of increase of electron internal energy. This result may help clarify differences in how the reconnection and turbulence communities quantify "dissipation".

Key Points:

- Time integrated volume averaged electromagnetic work does not formally or generally correspond to dissipation
- Due to small electron mass, time integrated volume averaged pressure strain and electromagnetic work are nearly equal for electrons
- Differences between instantaneous electromagnetic work and pressure strain can be considerable, but for electrons, these average to zero

Correspondence to:
Y. Yang,
yanyang@udel.edu

Citation:
Yang, Y., Adhikari, S., & Matthaeus, W. H. (2024). Electron dissipation and electromagnetic work. *Journal of Geophysical Research: Space Physics*, *129*, e2024JA033105. https://doi.org/10.1029/2024JA033105

Received 23 JUL 2024
Accepted 3 OCT 2024

1. Introduction

Energy dissipation in fluids and plasmas may be effectively defined as the conversion process by which macroscopic reservoirs of energy are transformed into heat. Mechanisms of energy dissipation for weakly collisional or collisionless plasma are of central importance for addressing long-standing fundamental problems in space and astrophysics. These include, for example, the acceleration of energetic particles and the heating of the solar corona and solar wind. Space plasmas frequently reside in (nearly) collisionless regimes, where the dissipation mechanisms are complex, not well understood and perhaps even controversial. In one of the most well-studied space plasmas, the solar wind (Bruno & Carbone, 2013), the collision length is of the order of 1 AU and collisions are typically too weak to establish a local equilibrium (Maxwellian distribution). In such cases the classical collisional approach becomes generally inapplicable, as do standard closures that describe dissipation in terms of fluid-scale variables and viscosity and resistivity.

Lacking the standard collisional closures, studies of plasma turbulence have shown increasing interest in quantifying collisionless dissipation. A useful approach to understand dissipation is to trace the flow of energy and examine energy conversion between different forms (Matthaeus et al., 2020). Temperature enhancement implies increase of thermal energy and to specifically track thermal energy production requires quantification of energy supplies from energy reservoirs for each species. Two widely invoked classes of conversion are the electric work on particles for species α, $\boldsymbol{j}_\alpha \cdot \boldsymbol{E}$ (Zenitani et al., 2011) and the pressure-strain interaction for species α, $-(\boldsymbol{P}_\alpha \cdot \nabla) \cdot \boldsymbol{u}_\alpha$ (Yang, Matthaeus, Parashar, Haggerty, et al., 2017; Yang, Matthaeus, Parashar, Wu, et al., 2017). It is trivial to obtain these channels from Vlasov-Maxwell equations. The time evolution of energies can be derived using the first three moments of the Vlasov equation, in conjunction with the Maxwell equations. One obtains (Braginskii, 1965; Chiuderi & Velli, 2015; Marshall, 1957; Yang, Matthaeus, Parashar, Haggerty, et al., 2017; Yang, Matthaeus, Parashar, Wu, et al., 2017)

$$\partial_t E_\alpha^f + \nabla \cdot \left(E_\alpha^f \boldsymbol{u}_\alpha + \boldsymbol{P}_\alpha \cdot \boldsymbol{u}_\alpha\right) = (\boldsymbol{P}_\alpha \cdot \nabla) \cdot \boldsymbol{u}_\alpha + \boldsymbol{j}_\alpha \cdot \boldsymbol{E}, \tag{1}$$

$$\partial_t E_\alpha^{th} + \nabla \cdot \left(E_\alpha^{th} \boldsymbol{u}_\alpha + \boldsymbol{h}_\alpha\right) = -(\boldsymbol{P}_\alpha \cdot \nabla) \cdot \boldsymbol{u}_\alpha, \tag{2}$$

$$\partial_t E^m + \frac{c}{4\pi}\nabla\cdot(\boldsymbol{E}\times\boldsymbol{B}) = -\boldsymbol{j}\cdot\boldsymbol{E}, \tag{3}$$

where the subscript $\alpha = e,p$ represents the particle species (electrons and protons); $E^m = \left(\boldsymbol{B}^2 + \boldsymbol{E}^2\right)/(8\pi)$ is the electromagnetic energy density, with $\boldsymbol{E}$, $\boldsymbol{B}$ the electric and magnetic fields; $E^f_\alpha = \frac{1}{2}\rho_\alpha \boldsymbol{u}_\alpha^2$ is the bulk flow energy density for species α, with mass density ρ_α and bulk flow velocity $\boldsymbol{u}_\alpha$; $E^{th}_\alpha = \frac{1}{2}m_\alpha \int_v (\boldsymbol{v}-\boldsymbol{u}_\alpha)\cdot(\boldsymbol{v}-\boldsymbol{u}_\alpha) f_\alpha \, \mathrm{d}^3 v$ is the internal (or thermal) energy, with mass m_α and velocity distribution function $f_\alpha(\boldsymbol{x},\boldsymbol{v})$; $\boldsymbol{P}_\alpha$ is the pressure tensor; $\boldsymbol{h}_\alpha$ is the heat flux vector; $\boldsymbol{j} = \sum_\alpha \boldsymbol{j}_\alpha$ is the total electric current density with $\boldsymbol{j}_\alpha = n_\alpha q_\alpha \boldsymbol{u}_\alpha$ the electric current density of species α; $n_\alpha(\boldsymbol{x})$ and q_α are the number density and the charge of species α, respectively.

As we can see the two channels play different roles: the electromagnetic work $\boldsymbol{j}\cdot\boldsymbol{E}$ measures the release of electromagnetic energy, while the pressure-strain interaction $-(\boldsymbol{P}_\alpha\cdot\nabla)\cdot\boldsymbol{u}_\alpha$ measures the increase of internal energy, which is validated in fully kinetic simulations (Pezzi et al., 2019; Yang et al., 2022). J. Burch et al. (2023) also reports the conversion of electromagnetic energy to electron kinetic energy by $\boldsymbol{j}\cdot\boldsymbol{E}$ and the ensuing conversion of electron beam energy to electron thermal energy via $-(\boldsymbol{P}_e\cdot\nabla)\cdot\boldsymbol{u}_e$ in a magnetotail reconnection region. We note for future reference that pressure strain can be decomposed into "compressive" ($p\theta$) and "incompressive" (PiD) ingredients (Yang et al., 2017).

The subtle relationship between these channels of conversion has motivated some discussion in the community concerning the role the electromagnetic work $\boldsymbol{j}\cdot\boldsymbol{E}$, which has been adopted widely to estimate "dissipation" and heating rates (Chasapis, Matthaeus, et al., 2018; Duan et al., 2020; Ergun et al., 2018; Lu et al., 2019; Phan et al., 2018; Pongkitiwanichakul et al., 2021; Vörös et al., 2019; Wan et al., 2012a, 2015; Wilder et al., 2017; Zenitani et al., 2011). This measure is of great importance in magnetic reconnection, where energy is initially concentrated in the magnetic field, and the electromagnetic work quantifies the release of energy from this magnetic reservoir. One often separates out the non-ideal part of the electric field $\boldsymbol{E}' = \boldsymbol{E} + \boldsymbol{u}_e/c \times \boldsymbol{B}$, and identifies the quantity $\boldsymbol{j}\cdot\boldsymbol{E}'$, which is the electromagnetic work in the electron frame (Zenitani et al., 2011) as irreversible dissipation.

Energy dissipation processes are, however, different for electrons and ions and hence it is reasonable to employ separate measures for them. However, this distinction is not quantified by the standard electromagnetic work $\boldsymbol{j}\cdot\boldsymbol{E}$ (Sitnov et al., 2018). In this sense, the electromagnetic work on particles for species α, $\boldsymbol{j}_\alpha\cdot\boldsymbol{E}$ might be more meaningful. However, as shown in Equation 1, $\boldsymbol{j}_\alpha\cdot\boldsymbol{E}$ is not in direct correspondence with either the internal energy increase or the temperature enhancement. Instead, the change of the internal energy takes place directly through the pressure-strain interaction, $-(\boldsymbol{P}_\alpha\cdot\nabla)\cdot\boldsymbol{u}_\alpha$, for both ions and electrons, a result that follows from the Vlasov-Maxwell theory (Bacchini et al., 2022; Bandyopadhyay et al., 2020a; Barbhuiya & Cassak, 2022; Cassak & Barbhuiya, 2022; Cassak et al., 2022; Chasapis, Yang, et al., 2018; Hellinger et al., 2022; Jiang et al., 2021; Sitnov et al., 2018; Yang, 2019; Yang, Matthaeus, Parashar, Haggerty, et al., 2017; Yang, Matthaeus, Parashar, Wu, et al., 2017; Zhong et al., 2019).

Although there is hardly any doubt that both electromagnetic work and pressure-strain interaction are key ingredients of energy conversion, many details are still under debate. For example, for some time there has been a discrepancy between the way that the collisonless reconnection community treats "dissipation" and the way that the plasma turbulence community treats the same quantity. On the one hand, in collisonless reconnection the electromagnetic work in the electron fluid frame, essentially the same as the Zenitani measure $\boldsymbol{j}\cdot\boldsymbol{E}'$, is treated as dissipation. Such studies, often employ high resolution Magnetosphere Multiscale (MMS) Mission data and intensively study collisionless physics at electron scales (J. L. Burch et al., 2016; Wilder et al., 2018; Bandyopadhyay et al., 2020b). The quantity $\boldsymbol{j}\cdot\boldsymbol{E}$ plays an essential role in such studies in the identification of release of energy from the magnetic field, which in fact is the dominant energy reservoir in the cases studied. In this situation it is a small step beyond to conclude that the energy so released is in fact *dissipated*. But is this latter conclusion an exact statement or is it a kind of shorthand for unresolved intermediate processes? The present paper represents an elaboration on this question and its resolution, which we hope attains some clarity.

A similar perspective has emerged in the collisionless plasma turbulence community. Keeping in mind that numerical simulation of collisonless turbulence has blossomed only in the past two decades (Bowers & Li, 2007; Howes, 2008; Parashar et al., 2009), for some time the association of dissipation with $\boldsymbol{j}\cdot\boldsymbol{E}$ was adopted, making contact with the reconnection community. For example, electromagnetic work is prominent in baseline studies of

cascade and intermittency (Karimabadi et al., 2013; Wan et al., 2012b), even though no dissipation function per se was discussed.

A different perspective (Yang et al., 2022; Yang, Matthaeus, Parashar, Haggerty, et al., 2017) emerged by consideration of the energy budget equations Equations 1–3 that emerge directly from Vlasov-Mawell system (Braginskii, 1965; Marshall, 1957). In turbulence studies, this led to the identification of the pressure strain interaction as the dissipation function for each species, a connection well confirmed in well resolved kinetic plasma numerical simulations (Pezzi et al., 2020; Yang et al., 2022). Application of this idea has led to improved clarity in analyzing plasma turbulence in the form of adaptation of von-Karman Howarth theory, the analysis of electron-proton heating ratios, and identification of compressive versus incompressive cascade dissipation channels (Roy et al., 2022).

The purpose of the present paper is to clarify the relationships between the above perspectives, especially for electrons.

2. Theoretical Background

The first vector moment of the Vlasov equation for species α gives rise to the momentum equation

$$\rho_\alpha \frac{\mathrm{d}\boldsymbol{u}_\alpha}{\mathrm{d}t} = -\nabla\cdot\boldsymbol{P}_\alpha + n_\alpha q_\alpha\left(\boldsymbol{E}+\frac{1}{c}\boldsymbol{u}_\alpha\times\boldsymbol{B}\right). \tag{4}$$

As discussed in Wang and Yang (2023), we first look at the momentum equation for electrons. In the limit of massless electrons, the inertial term on the left-hand side is negligible. The remaining terms represent the balance of the non-ideal electric field $\boldsymbol{E}' = \boldsymbol{E}+\boldsymbol{u}_e/c\times\boldsymbol{B}$ and the electron pressure tensor gradient,

$$n_e q_e \boldsymbol{E}' = \nabla\cdot\boldsymbol{P}_e. \tag{5}$$

On computing the inner product of Equation 5 and the electron bulk velocity, the left-hand side becomes $\boldsymbol{j}_e\cdot\boldsymbol{E}' = \boldsymbol{j}_e\cdot\boldsymbol{E}$ and the right-hand term becomes $\boldsymbol{u}_e\cdot(\nabla\cdot\boldsymbol{P}_e) = \nabla\cdot(\boldsymbol{P}_e\cdot\boldsymbol{u}_e) - (\boldsymbol{P}_e\cdot\nabla)\cdot\boldsymbol{u}_e$. The spatial transport terms, for example, the second terms on the left-hand side of Equations 1–3 and $\nabla\cdot(\boldsymbol{P}_e\cdot\boldsymbol{u}_e)$ are globally conservative and cancel out under certain boundary conditions, for example, periodic. Therefore, one can obtain the equivalence of the two energy conversion channels,

$$\langle \boldsymbol{j}_e\cdot\boldsymbol{E}'\rangle = \langle \boldsymbol{j}_e\cdot\boldsymbol{E}\rangle = \langle -(\boldsymbol{P}_e\cdot\nabla)\cdot\boldsymbol{u}_e\rangle, \tag{6}$$

where brackets indicate an appropriate volume average. That is, the magnetic energy is converted into electron bulk flow energy through $\langle \boldsymbol{j}_e\cdot\boldsymbol{E}\rangle$, which is completely converted, at this level of approximation, into electron thermal energy through $\langle -(\boldsymbol{P}_e\cdot\nabla)\cdot\boldsymbol{u}_e\rangle$.

It is possible to conclude, then, that for massless electrons, the resultant bulk flow energy gain is negligible and all magnetic energy that is deposited on average into the electron population ends up in the form of electron thermal energy. In this case, the global properties of the two channels do not differ in any important manner. However, one cannot assert their point-wise (or local) equivalence since the transport terms are likely to exert significant influence (Du et al., 2020; Fadanelli et al., 2021).

Electrons are assumed to be massless as deriving Equation 6. Such assumption is not justified physically for protons or other heavy ion species. Therefore, no such relation as Equation 6 can be obtained for protons. Since the pressure-strain interaction $\langle -(\boldsymbol{P}_p\cdot\nabla)\cdot\boldsymbol{u}_p\rangle$ can remove energy from bulk fluid flow, the amount of energy deposited into proton thermal energy is limited by the reservoir of proton bulk fluid flow energy, which in turn can be supplied by electromagnetic energy through $\langle \boldsymbol{j}_p\cdot\boldsymbol{E}\rangle$. Larger bulk fluid flow energy supply through $\langle \boldsymbol{j}_p\cdot\boldsymbol{E}\rangle$ indicates that more energy could overflow into thermal energy through $\langle -(\boldsymbol{P}_p\cdot\nabla)\cdot\boldsymbol{u}_p\rangle$.

Given that the above physical arguments are based approximations of small electron mass and the existence of suitable averaging volume, we now turn to numerical results from PIC simulations of turbulence and reconnection for corroboration.

3. Data

We present data from 2.5D fully kinetic PIC simulations of turbulence and reconnection, employing the P3D code (Zeiler et al., 2002). These simulations of an electron-proton plasma have been used in previous related studies Yang et al. (2022, 2023, 2024), Bandyopadhyay et al. (2023), and Adhikari et al. (2023, 2024). As usual, "2.5D" indicates that there are three components of the dependent field vectors and a two-dimensional (2D) spatial grid, so that the phase space coordinates are $\left(x, y, v_x, v_y, v_z\right)$. Normalization in P3D is largely "proton-based", with number density normalized to a reference value n_r, mass normalized to proton mass m_p, charge normalized to proton charge e, and magnetic field normalized to a reference field B_r. Length is normalized to the proton inertial length d_p, time normalized to the proton cyclotron time ω_{cp}^{-1}, and velocity normalized to the equivalent reference Alfvén speed $V_{Ar} = B_r/\left(\mu_0 m_p n_r\right)^{1/2}$.

Both turbulence and reconnection simulations are performed in a square periodic domain with 4096^2 spatial grid points. For numerical expediency both simulations employ artificially low values of the proton to electron mass ratio, $m_p/m_e = 25$, and the speed of light, $c = 15\ V_{Ar}$.

For simulation of turbulence we use a box of size $L = 150\ d_p$ with 3,200 particles of each species per cell ($\sim 1.07 \times 10^{11}$ total particles). The run is a decaying initial value problem, starting with uniform densities and temperatures for both species. A uniform magnetic field, $B_0 = 1.0$, is directed out of, and normal to, the plane. The initial $\boldsymbol{v}$ and $\boldsymbol{b}$ fluctuations are transverse to B_0 (corresponding in linear theory to a small amplitude "Alfvén mode") in Fourier wavevectors $2 \leq |\boldsymbol{k}| \leq 4$ with random phases and prescribed amplitudes. The initial fluctuation energy, flow plus magnetic, is $E = 0.1$, plasma beta $\beta = 0.6$ and the normalized cross helicity σ_c is negligible.

Similarly, reconnection simulation uses a box of size $L = 204.8\ d_p$ with 100 particles of each species per cell ($\sim 3.4 \times 10^9$ total particles). The simulation is initialized using a double Harris equilibrium with a half-width of 3 d_p for the current sheet and a background density of 0.2. The initial ion and electron temperatures are set at 1.25 and 0.25 respectively such that $T_p/T_e = 5$. A sinusoidal perturbation is used to initiate reconnection and the system is evolved until the quasi-steady phase of reconnection attenuates. Multiple simulations with different out-of-plane magnetic fields (guide fields) are analyzed in this study. While the overall behavior of energy transfer channels is the same in all these simulations, for consistency only the results from $B_g = 1$ run with $\beta_p = 0.25$ and $\beta_e = 0.05$ are presented in this paper.

Both the simulations are run for about $450 t\omega_{cp}$ and the data output is saved at every $0.5 t\omega_{cp}$ for turbulence and $1 t\omega_{cp}$ for reconnection. Prior to analyses, we recursively smooth the raw simulation parameters four times over a width of four cells to reduce the noise inherent in the PIC plasma algorithm. This smoothing corresponds to filtering scales of $\ell = 0.12 d_i$ and $0.2 d_i$ for simulations of turbulence and reconnection respectively, and is based on a trial of multiple smoothing options such that it does not largely alter the structures.

The proton-to-electron mass ratio $m_p/m_e = 25$ is very small compared to the actual value of 1,836. It is well known that a small mass ratio might introduce some unrealistic effects (Edyvean et al., 2024). However, it is shown previously that the electron mass has insignificant effect on the large scale evolution (Ricci et al., 2002) and therefore sufficient to separate the different behaviors of $\boldsymbol{j}_\alpha \cdot \boldsymbol{E}$ and $-(\boldsymbol{P}_\alpha \cdot \nabla) \cdot \boldsymbol{u}_\alpha$ for electrons and protons.

4. Results

4.1. Turbulence

We first consider energy balances in the turbulence run. Figure 1 shows the energy balance for the turbulence run by comparing the time evolution of the changes in electromagnetic and thermal energies with the cumulative time-integrated values of $\langle \boldsymbol{j} \cdot \boldsymbol{E} \rangle$ and pressure-strain interaction $\langle -(\boldsymbol{P} \cdot \nabla) \cdot \boldsymbol{u} \rangle$ of individual species. The integrals have been computed after $9 t\omega_{cp}$ to remove the effect of large initial oscillations in the out-of-plane current. The brackets $\langle \cdots \rangle$ signify an average over the entire box. The global average of the time evolution equations (Equations 2 and 3) are satisfied to a great degree. For example,: the cumulative time integrated $\langle -\boldsymbol{j} \cdot \boldsymbol{E} \rangle$ and the change of the electromagnetic energy $\langle \delta E^m \rangle$ are almost identical, as expected. The change in internal energy for each species $\langle \delta E^{th} \rangle$ is instead related to their time integrated pressure strain interaction $\langle -(\boldsymbol{P} \cdot \nabla) \cdot \boldsymbol{u} \rangle$ as shown in Figure 1.

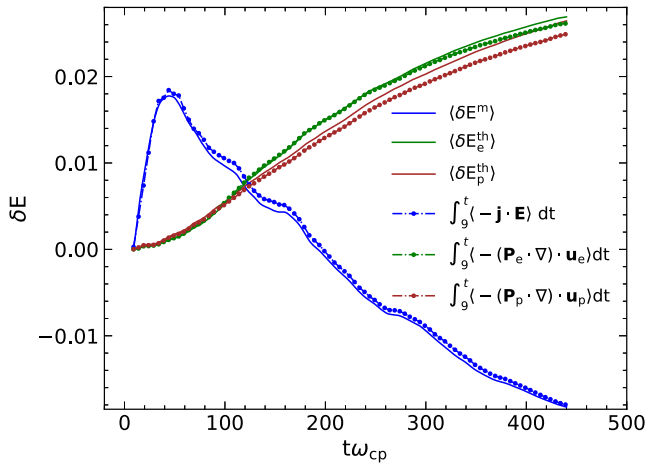

Figure 1. Time evolution of the changes of electromagnetic and thermal energies versus time-integrated $\langle -\boldsymbol{j}\cdot\boldsymbol{E}\rangle$, $\langle -(\boldsymbol{P}_e\cdot\nabla)\cdot\boldsymbol{u}_e\rangle$, $\langle -(\boldsymbol{P}_p\cdot\nabla)\cdot\boldsymbol{u}_p\rangle$ for turbulence simulation. Here the change of energy is defined as $\delta E(t) = E(t) - E(9)$ and the integral is computed over time $[9,\ t]$ in units of ω_{cp}^{-1}.

In Figure 2 we show the change in bulk flow energies $\langle \delta E^f \rangle$ for the turbulence run. For protons $\langle \delta E_p^f \rangle$ matches well with the time-integrated sum of the pressure strain interaction and the electromagnetic work $\langle \boldsymbol{j}_p\cdot\boldsymbol{E} + (\boldsymbol{P}_p\cdot\nabla)\cdot\boldsymbol{u}_p\rangle$. The differences observed in these curves are mainly due to the effect of the limited particles per cell, an artifact of PIC simulations, and also due to the time integration inaccuracy. For electrons, there is comparatively a larger discrepancy between the change in the flow energy and the time-integrated sum of electron pressure strain interaction and electron electromagnetic work $\langle \boldsymbol{j}_e\cdot\boldsymbol{E} + (\boldsymbol{P}_e\cdot\nabla)\cdot\boldsymbol{u}_e\rangle$. This is likely associated with higher frequency signals in the electron current and the electron pressure tensor.

In the turbulence simulation under consideration, the change of the electron flow energy is almost zero. The sum of the time integrated $\langle \boldsymbol{j}_e\cdot\boldsymbol{E}\rangle$ and $\langle(\boldsymbol{P}_e\cdot\nabla)\cdot\boldsymbol{u}_e\rangle$ oscillates about zero until about $100t\omega_{cp}$ and roughly stays flat at about $\sim$0.003 throughout the simulation. It is worth comparing this amplitude with the individual time integral of $\langle \boldsymbol{j}_e\cdot\boldsymbol{E}\rangle$ and $\langle(\boldsymbol{P}_e\cdot\nabla)\cdot\boldsymbol{u}_e\rangle$ as shown in Figure 2. Clearly, the time integral of $\langle \boldsymbol{j}_e\cdot\boldsymbol{E}\rangle$ and $\langle(\boldsymbol{P}_e\cdot\nabla)\cdot\boldsymbol{u}_e\rangle$ seem to be anticorrelated to each other and the small non-zero sum accounts for the initial oscillations in the electron current and electric field. For protons, no anticorrelation is observed between $\langle \boldsymbol{j}_p\cdot\boldsymbol{E}\rangle$ and $\langle(\boldsymbol{P}_p\cdot\nabla)\cdot\boldsymbol{u}_p\rangle$, as the sum is non zero. Note that most of the dynamics occurs at the expense of ion flow energy.

Before we dive further into the global features of the pressure-strain interaction and electromagnetic work for electrons, we explore the local structures of these quantities. In Figure 3, we show the 2D plots of electron pressure-strain interaction $(\boldsymbol{P}_e\cdot\nabla)\cdot\boldsymbol{u}_e$ and electron electromagnetic work $\boldsymbol{j}_e\cdot\boldsymbol{E}$ along with the out-of-plane electron current density j_{ez} and contours of magnetic flux at $t\omega_{cp} = 163$, after the mean square current has peaked and turbulence is fully developed. As shown on the leftmost plot in Figure 3, the electron current sheets are much more localized with almost no current inside the magnetic islands. The middle and the rightmost plots show that the pressure-strain interaction and the electromagnetic work are also localized along the current sheets. One should keep in mind that these quantities are prone to the particle noise, an artifact of PIC simulations. A proper

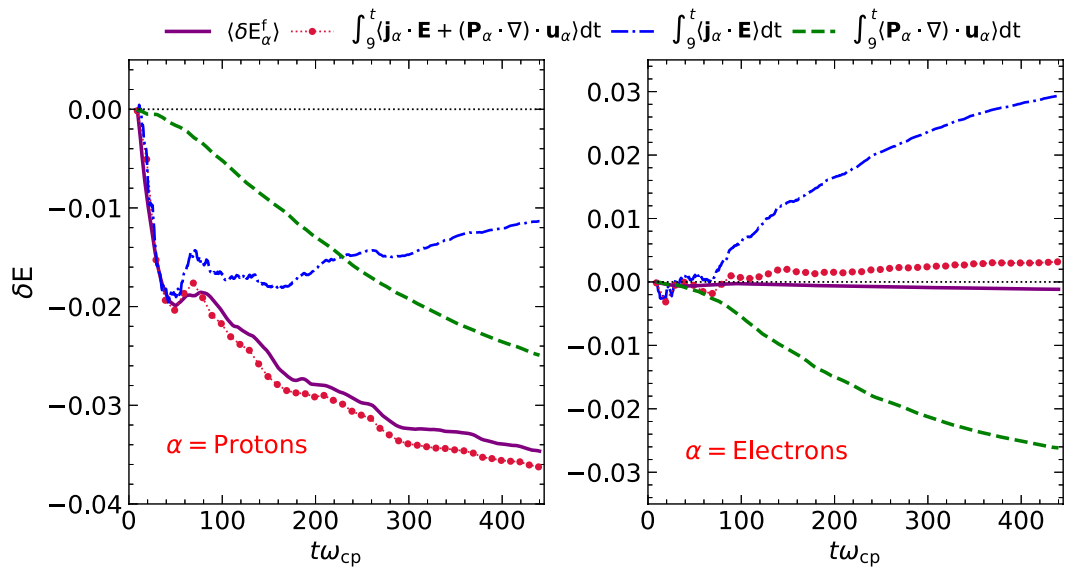

Figure 2. Time evolution of the change in flow energy along with the cumulative time-integrated $\langle \boldsymbol{j}_\alpha\cdot\boldsymbol{E} + (\boldsymbol{P}_\alpha\cdot\nabla)\cdot\boldsymbol{u}_\alpha\rangle$, $\langle \boldsymbol{j}_\alpha\cdot\boldsymbol{E}\rangle$, and $\langle(\boldsymbol{P}_\alpha\cdot\nabla)\cdot\boldsymbol{u}_\alpha\rangle$ for protons (left) and electrons (right) in turbulence simulation. A dotted horizontal line at $\delta E = 0$ is drawn for reference.

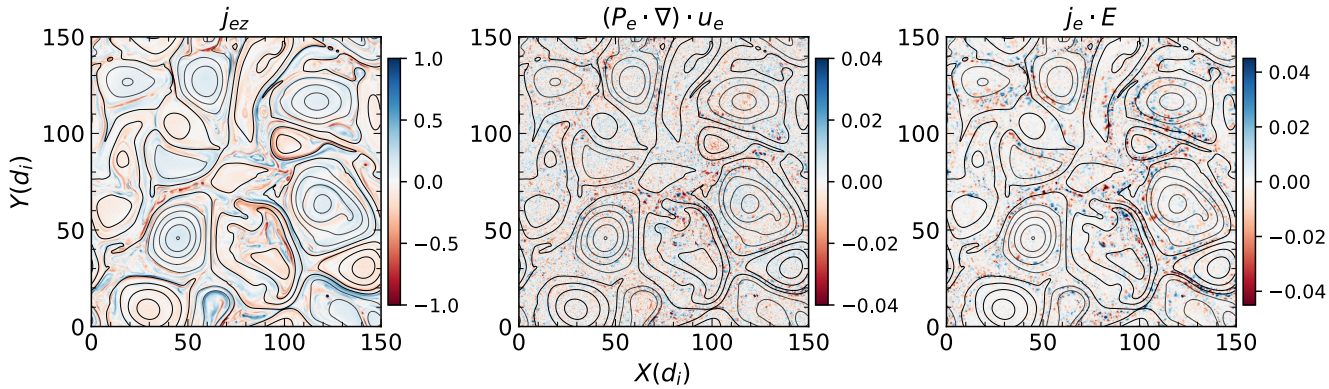

Figure 3. Overview of the electron out-of-plane current density j_{ez}, electron pressure-strain interaction $(\boldsymbol{P}_e \cdot \nabla) \cdot \boldsymbol{u}_e$, and electron electromagnetic work $\boldsymbol{j}_e \cdot \boldsymbol{E}$ for turbulence simulation at $t\omega_{ci} = 163$.

time averaging (Haggerty et al., 2017) over a high cadence data can minimize the noise effects, but since this study does not focus on local effects, such time averaging is not performed here.

To investigate the degree and nature of the validity of Equation 6 further, we plot the detailed time evolution of the global averaged electron electromagnetic work $\langle \boldsymbol{j}_e \cdot \boldsymbol{E} \rangle$ and electron pressure strain interaction $\langle -(\boldsymbol{P}_e \cdot \nabla) \cdot \boldsymbol{u}_e \rangle$ starting $9t\omega_{cp}$ in Figure 4. For clarity, data points after every $10t\omega_{cp}$ are plotted. Clearly, for $\langle \boldsymbol{j}_e \cdot \boldsymbol{E} \rangle$, there are some big oscillations in the initial phase. As a result, the instantaneous values of $\langle \boldsymbol{j}_e \cdot \boldsymbol{E} \rangle$ and $\langle -(\boldsymbol{P}_e \cdot \nabla) \cdot \boldsymbol{u}_e \rangle$ do not agree well with each other. However, as seen previously, the cumulative time integral of these quantities agree much better since these oscillations are canceled in the cumulative sum.

4.2. Reconnection

Next, we explore these features in the guide-field Harris reconnection run. Figure 5 shows the time evolution of the energies for reconnection in the same format as Figure 1. One should keep in mind that the initial conditions for these turbulence and reconnection simulation runs are totally different, and their dynamics evolve very differently in the two cases. For example,: the evolution phase of reconnection is completely different than turbulence, where typically the system immediately undergoes an initial exchange of energy between the ion-flow and magnetic field (see, e.g. (Cho & Vishniac, 2000),). For reconnection, no such exchange occurs and until about $200t\omega_{cp}$ reconnection has not started. Once reconnection initiates, electromagnetic energy gets transferred mostly to thermal energy (Adhikari et al., 2021). However, the change in electromagnetic energy $\langle \delta E^m \rangle$ very closely follows the time integral of the electromagnetic work $\langle -\boldsymbol{j} \cdot \boldsymbol{E} \rangle$. Similarly, the change in the thermal energies $\langle \delta E^{th} \rangle$ for each species and the time integral of the respective pressure strain interactions $\langle -(\boldsymbol{P} \cdot \nabla) \cdot \boldsymbol{u} \rangle$ are almost equal, except for a slight variation seen for the electrons.

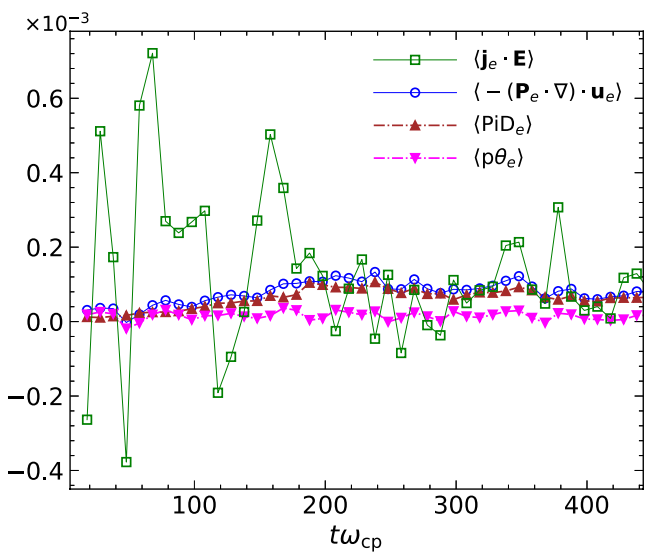

Figure 4. Time evolution of $\langle \boldsymbol{j}_e \cdot \boldsymbol{E} \rangle$; $\langle p\theta_e \rangle$, $\langle PiD_e \rangle$, and $\langle -(\boldsymbol{P}_e \cdot \nabla) \cdot \boldsymbol{u}_e \rangle$ for the 2.5D turbulence simulation. For clarity data points after every $10t\omega_{cp}$ are plotted.

In Figure 6, we show the time evolution of the change in the flow energy for reconnection along with the time integrated $\langle \boldsymbol{j}_\alpha \cdot \boldsymbol{E} \rangle$, $\langle (\boldsymbol{P}_\alpha \cdot \nabla) \cdot \boldsymbol{u}_\alpha \rangle$, and their sum. The flow energy evolution equations are once again very well satisfied. While the evolution of the energies is different between these turbulence and reconnection runs, one similarity is the small change in the electron flow energy, which results in an anticorrelation between $\langle \boldsymbol{j}_e \cdot \boldsymbol{E} \rangle$ and $\langle (\boldsymbol{P}_e \cdot \nabla) \cdot \boldsymbol{u}_e \rangle$. In reconnection, the discrepancy between time integrated $\langle \boldsymbol{j}_e \cdot \boldsymbol{E} + (\boldsymbol{P}_e \cdot \nabla) \cdot \boldsymbol{u}_e \rangle$ and change in δE_e^f is much smaller compared to turbulence. This is because in reconnection the system evolves slowly, and we do not observe huge oscillations in the electron current.

Figure 7 shows the real space plots of the out-of-plane current density, pressure strain interaction and electromagnetic work for electrons at $t\omega_{ci} = 345$, during the quasi-steady phase of reconnection when the

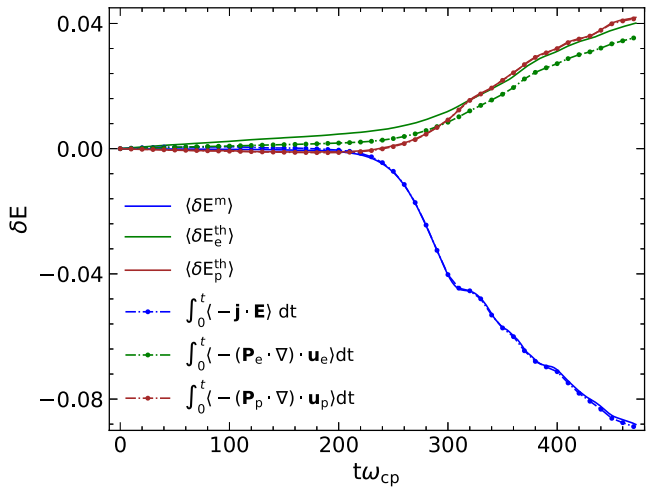

Figure 5. Time evolution of the changes of electromagnetic and thermal energies versus cumulative time-integrated $\langle -\boldsymbol{j}\cdot\boldsymbol{E}\rangle$, $\langle -(\boldsymbol{P}_e\cdot\nabla)\cdot\boldsymbol{u}_e\rangle$, $\langle -(\boldsymbol{P}_p\cdot\nabla)\cdot\boldsymbol{u}_p\rangle$ for reconnection simulation with a guide field of unity. Here the change of energy is defined as $\delta E(t) = E(t) - E(0)$ and the cumulative integral is computed over time $[0,\ t]$ in units of ω_{cp}^{-1}.

maximum value of the mean square current has already been achieved in the simulation. Compared to the turbulence case, the system is filled with only two reconnection sites in the reconnection simulation and two corresponding magnetic islands. The electron pressure-strain interaction and the electron magnetic work are also mostly localized along the reconnection sites with some structures along the outflow surrounding the magnetic islands. It is evident that, a point wise local anticorrelation between $(\boldsymbol{P}_e\cdot\nabla)\cdot\boldsymbol{u}_e$ and $\boldsymbol{j}_e\cdot\boldsymbol{E}$ is not realized since the transport terms in Equations 1–3 can be locally significant.

In Figure 8, we plot the instantaneous values of $\langle \boldsymbol{j}_e\cdot\boldsymbol{E}\rangle$ and $\langle -(\boldsymbol{P}_e\cdot\nabla)\cdot\boldsymbol{u}_e\rangle$ in reconnection, which, free of large initial oscillations, agree very well. This implies that Equation 6 may be valid pointwise in time for slowly evolving systems while it may not be as well satisfied in rapidly evolving systems. Nevertheless, since electron flow energy is insignificant in plasma systems, the time integral of $\langle \boldsymbol{j}_e\cdot\boldsymbol{E}\rangle$ and $\langle(\boldsymbol{P}_e\cdot\nabla)\cdot\boldsymbol{u}_e\rangle$ are always anticorrelated.

5. Discussion and Conclusions

In spite of the significant advances in both communities, the dichotomy between dissipation as viewed in reconnection and turbulence studies has persisted. The present paper has attempted to at least partially elucidate the relationship between these perspectives. To achieve this we began by recapitulating some of the results from Yang et al. (2022) that demonstrated that the pressure strain interactions act as the species dissipation functions in collisionless plasma. Apart from reviewing that result, we also showed the reconciliation of the terms in Equations 1–3 employing improved time cadence data, thus improving the accuracy of the results.

It becomes immediately apparent for the turbulence simulation that the time integration of volume averaged electromagnetic work does not correspond to dissipation, while pressure-strain interaction accounts accurately for both proton and electron internal energy increases. Meanwhile the electromagnetic work accounts well for an epoch of field line stretching at early times, with associated increase of magnetic energy and loss of proton fluid kinetic energy. Electrons do not act independently in this period, and the heating (internal energy increase) of

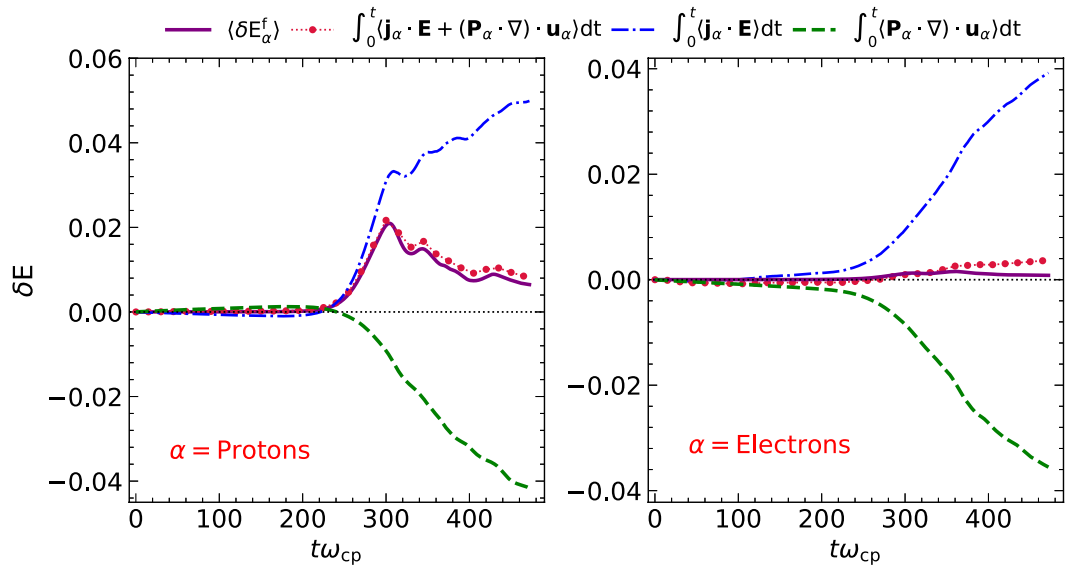

Figure 6. Time evolution of the change in flow energy along with the cumulative time-integrated $\langle \boldsymbol{j}_\alpha\cdot\boldsymbol{E} + (\boldsymbol{P}_\alpha\cdot\nabla)\cdot\boldsymbol{u}_\alpha\rangle$, $\langle \boldsymbol{j}_\alpha\cdot\boldsymbol{E}\rangle$, and $\langle(\boldsymbol{P}_\alpha\cdot\nabla)\cdot\boldsymbol{u}_\alpha\rangle$ for protons (left) and electrons (right) in reconnection simulation. A dotted horizontal line at $\delta E = 0$ is drawn for reference.

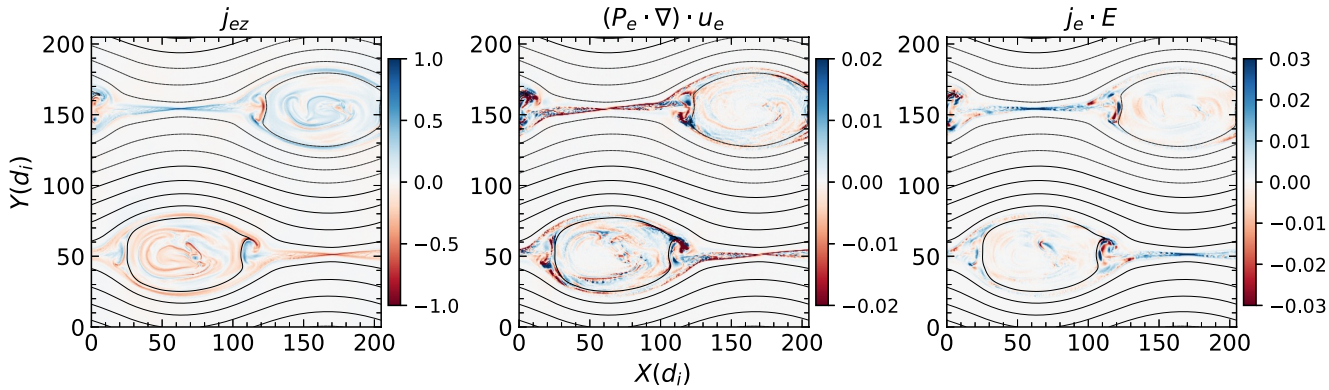

Figure 7. Overview of the electron out-of-plane current density j_{ez}, electron pressure-strain interaction $(\boldsymbol{P}_e \cdot \nabla) \cdot \boldsymbol{u}_e$, and electron electromagnetic work $\boldsymbol{j}_e \cdot \boldsymbol{E}$ for reconnection simulation at $t\omega_{ci} = 345$.

electrons and protons are temporarily very nearly equal. At later times (after the field line stretching period) the proton fluid kinetic energy receives a nearly constant (and slightly increasing) input from electromagnetic work. A likely interpretations is that this is a consequence of plasma jets generated by reconnection of adjacent magnetic islands (Servidio et al., 2010).

During this time (after $t\omega_{cp} \sim 120$) effect of electromagnetic work on electrons differs greatly from that on protons. There is for example, a dramatic increase in production of electron flow energy caused by electromagnetic work, an effect much greater than the analogous effect on protons in this period. There is also a very similar dramatic increase in the production of electron internal energy, which of course must occur at the expense of electron flow energy, as is evident in Figure 2. A significant consequence, seen also in this figure, is that the *sum* of these effects leaves the electron flow kinetic energy very nearly constant for hundreds of proton cyclotron times. The only way this can happen is that the time-integrated volume average effects on electrons of electromagnetic work and pressure strain are very nearly in balance, that is, in a time-averaged sense, $\langle \boldsymbol{j}_e \cdot \boldsymbol{E} \rangle = \langle -(\boldsymbol{P}_e \cdot \nabla) \cdot \boldsymbol{u}_e \rangle$ as stated in Equation 6. This may be viewed as a main conclusion of the paper: that, apart from startup transients in fully developed turbulence, the aggregate time averaged dissipation by electrons may be equivalently viewed as either due to pressure strain, or due to electromagnetic work. The former is an exact statement; the latter a very good approximation, with the above caveats.

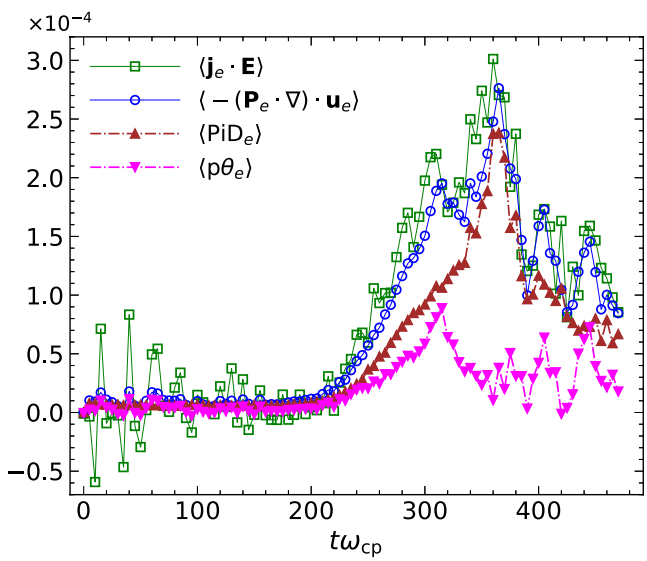

Figure 8. Time evolution of $\langle \boldsymbol{j}_e \cdot \boldsymbol{E} \rangle$; $\langle p\theta_e \rangle$, $\langle PiD_e \rangle$, and $\langle -(\boldsymbol{P}_e \cdot \nabla) \cdot \boldsymbol{u}_e \rangle$ for reconnection simulation. For clarity data points after every $5t\omega_{cp}$ are plotted.

It must be emphasized that this conclusion does not state that the underlying quantities are *pointwise* equal, or even equal in the spatial average at every time instant. One might note, for example, that based largely on kinetic plasma turbulence simulations, it has been well established that small scale features such as current sheets, vortices and measures of non-Maxwellianity (Greco et al., 2012; Parashar & Matthaeus, 2016; Servidio et al., 2012) tend to be clustered in specific regions, often near neutral points. This feature, which can be termed *regional correlation*, apparently applies as well to measures of plasma energy conversion and dissipation and can be quantified using two point correlation analysis (Yang et al., 2019). Apparently, this juxtaposition of kinetic effects in space carries over to the time domain as well, as can be seen, for quantities of present interest, by inspection of Figure 4. Here one may observe the time histories of the volume integrated electron pressure strain and the electromagnetic work on electrons. It is already shown above that the time integrals of these quantities follow each other rather closely. But in Figure 4 it is clear that at equal times these quantities may differ considerably. Note that the separate contributions of the time dependent volume averaged compressive $(p\theta_e)$ and incompressive (PiD_e) ingredients of pressure strain interaction (Yang, Matthaeus, Parashar, Haggerty, et al., 2017) are shown as additional traces in Figure 4. By inspection, one can verify that the compressive part is the much weaker of the two.

The results and conclusions for the reconnection case are very much in parallel to the turbulence case, with differences in the details, as shown in Figures 5 and 6. The time integrated pressure strain interactions agree quite well with the time histories of changes in the respective thermal energies, as was seen for the turbulence cases. While the results agree well for both species, it is curious that for the reconnection run, the greater discrepancy between integrated pressure strain and internal energy change occurs for the protons. In the turbulence case, the agreement between time integrated pressure strain and internal energy change for protons is slightly better than the agreements for the electrons. It is interesting to note that in Figure 6 the electromagnetic generation of proton flow energy is much more dramatic in the reconnection case than what was seen in the turbulence case. This clearly corresponds to the formation of large, energetic reconnection outflow jets.

A more significant difference in the turbulence and reconnection analyses is seen in the detailed time history of volume averaged electron pressure strain and similarly averaged electomagnetic work on electrons, shown in Figure 8. As in the case of turbulence, we already established that the respective time integrated quantities agree well with Equation 6. However, here, except for some large oscillatory differences at early time, for the reconnection case the agreement is much better between instantaneous values of volume averaged quantities than it is for the turbulence case. There remain modest quantitative differences, but the large oscillatory discrepancies are much less in Figure 8 than in Figure 4.

It is worth mentioning that this analysis has also been performed in two additional simulations of turbulence with different plasma beta $\beta = (0.3, 1.2)$, and four additional simulations of reconnection with different out-of-plane guide fields $Bg = (0, 0.1, 0.5, 2)$ and the results are consistent with those shown here and therefore independent of these parameters. In addition, for systems with real proton to electron mass ratio of 1,836, the change in electron flow energy becomes much smaller compared to the proton flow energy. As a result, we anticipate that the discrepancy between the electron pressure-strain interaction and electron electromagnetic work will be further reduced.

In summary we have shown that the volume averaged relation for electrons $\langle \boldsymbol{j}_e \cdot \boldsymbol{E} \rangle = \langle -(\boldsymbol{P}_e \cdot \nabla) \cdot \boldsymbol{u}_e \rangle$ is very well satisfied in a time integrated sense for reconnection cases and also for turbulence cases after a startup transient. As for detailed time variations, in turbulence there are relatively large discrepancies between the volume averaged electromagnetic work and the volume averaged pressure strain for electrons and these persist for the entire simulations. Standard reconnection cases are much quieter in this respect, and the time dependent discrepancies between these two important measures are much smaller except for early transients that are likely of numerical origin. We are hopeful that these results may contribute to a certain level of clarification regarding differences in the way "dissipation"is looked at in the reconnection and turbulence communities.

Data Availability Statement

The turbulence and reconnection simulation data used in the study are available at Yang et al. (2022, 2023, 2024) and Adhikari et al. (2023, 2024).

Acknowledgments
This research is partially supported by the MMS Theory, Modeling and Data Analysis team under NASA Grant 80NSSC19K0565, by the NASA LWS program under grants 80NSSC20K0198 and 80NSSC22K1020, and a subcontract from the New Mexico consortium 655–001, a NASA Heliophysics MMS-GI grant through a Princeton subcontract SUB0000517, and by the National Science Foundation Solar Terrestrial Program grant AGS-2108834. This research was also supported by the International Space Science Institute (ISSI) in Bern, through ISSI International Team projects #556 (Cross-scale energy transfer in space plasmas) and #23-588 ("Unveiling energy conversion and dissipation in non-equilibrium space plasmas"). We would like to acknowledge high-performance computing support from Cheyenne (doi:10.5065/D6RX99HX) and Derecho (https://doi.org/10.5065/qx9a-pg09) provided by NCAR's Computational and Information Systems Laboratory, sponsored by the National Science Foundation. We are particularly grateful to Sylvie Yang Jin (金浠言) for cooperation and assisting the lead author in completing this research.

References

Adhikari, S., Parashar, T., Shay, M., Matthaeus, W., Pyakurel, P., Fordin, S., et al. (2021). Energy transfer in reconnection and turbulence. *Physical Review*, *104*(6), 065206. https://doi.org/10.1103/physreve.104.065206

Adhikari, S., Shay, M. A., Parashar, T. N., Matthaeus, W. H., Pyakurel, P. S., Stawarz, J. E., & Eastwood, J. P. (2023). Effect of a guide field on the turbulence like properties of magnetic reconnection. *Physics of Plasmas*, *30*(8), 082904. https://doi.org/10.1063/5.0150929

Adhikari, S., Yang, Y., Matthaeus, W. H., Cassak, P. A., Parashar, T. N., & Shay, M. A. (2024). Scale filtering analysis of kinetic reconnection and its associated turbulence. *Physics of Plasmas*, *31*(2), 020701. https://doi.org/10.1063/5.0185132

Bacchini, F., Pucci, F., Malara, F., & Lapenta, G. (2022). Kinetic heating by Alfvén waves in magnetic shears. *Physical Review Letters*, *128*(2), 025101. https://doi.org/10.1103/physrevlett.128.025101

Bandyopadhyay, R., Matthaeus, W. H., Parashar, T. N., Yang, Y., Chasapis, A., Giles, B. L., et al. (2020a). Statistics of kinetic dissipation in the earth's magnetosheath: MMS observations. *Physical Review Letters*, *124*(25), 255101. https://doi.org/10.1103/PhysRevLett.124.255101

Bandyopadhyay, R., Matthaeus, W. H., Parashar, T. N., Yang, Y., Chasapis, A., Giles, B. L., et al. (2020b). Statistics of kinetic dissipation in the earth's magnetosheath: MMS observations. *Physical Review Letters*, *124*(25), 255101. https://doi.org/10.1103/PhysRevLett.124.255101

Bandyopadhyay, R., Yang, Y., Matthaeus, W. H., Parashar, T. N., Roytershteyn, V., Chasapis, A., et al. (2023). Collisional-like dissipation in collisionless plasmas. *Physics of Plasmas*, *30*(8), 080702. https://doi.org/10.1063/5.0146986

Barbhuiya, M. H., & Cassak, P. A. (2022). Pressure-strain interaction. III. Particle-in-cell simulations of magnetic reconnection. *Physics of Plasmas*, *29*(12), 122308. https://doi.org/10.1063/5.0125256

Bowers, K., & Li, H. (2007). Spectral energy transfer and dissipation of magnetic energy from fluid to kinetic scales. *Physical Review Letters*, *98*(3), 035002. https://doi.org/10.1103/PhysRevLett.98.035002

Braginskii, S. I. (1965). Transport processes in a plasma. *Reviews of plasma physics*, *1*, 205–311.

Bruno, R., & Carbone, V. (2013). The solar wind as a turbulence laboratory. *Living Reviews in Solar Physics*, *10*(1), 2. https://doi.org/10.12942/lrsp-2013-2

Burch, J., Genestreti, K., Heuer, S., Chasapis, A., Torbert, R., Gershman, D., et al. (2023). Electron energy dissipation in a magnetotail reconnection region. *Physics of Plasmas*, *30*(8), 082903. https://doi.org/10.1063/5.0153628

Burch, J. L., Torbert, R. B., Phan, T. D., Chen, L.-J., Moore, T. E., Ergun, R. E., et al. (2016). Electron-scale measurements of magnetic reconnection in space. *Science*, *352*(6290), aaf2939. Retrieved from https://www.science.org/doi/abs/10.1126/science.aaf2939

Cassak, P. A., & Barbhuiya, M. H. (2022). Pressure-strain interaction. I. On compression, deformation, and implications for Pi-D. *Physics of Plasmas*, *29*(12), 122306. https://doi.org/10.1063/5.0125248

Cassak, P. A., Barbhuiya, M. H., & Weldon, H. A. (2022). Pressure-strain interaction. II. Decomposition in magnetic field-aligned coordinates. *Physics of Plasmas*, *29*(12), 122307. https://doi.org/10.1063/5.0125252

Chasapis, A., Matthaeus, W., Parashar, T., Wan, M., Haggerty, C., Pollock, C., et al. (2018a). In situ observation of intermittent dissipation at kinetic scales in the earth's magnetosheath. *The Astrophysical Journal Letters*, *856*(1), L19. https://doi.org/10.3847/2041-8213/aaadf8

Chasapis, A., Yang, Y., Matthaeus, W., Parashar, T., Haggerty, C., Burch, J., et al. (2018b). Energy conversion and collisionless plasma dissipation channels in the turbulent magnetosheath observed by the magnetospheric multiscale mission. *The Astrophysical Journal*, *862*(1), 32. https://doi.org/10.3847/1538-4357/aac775

Chiuderi, C., & Velli, M. (2015). *Basics of plasma astrophysics*. Springer.

Cho, J., & Vishniac, E. T. (2000). The anisotropy of magnetohydrodynamic alfvénic turbulence. *The Astrophysical Journal*, *539*(1), 273–282. https://doi.org/10.1086/309213

Du, S., Zank, G. P., Li, X., & Guo, F. (2020). Energy dissipation and entropy in collisionless plasma. *Physical Review*, *101*(3), 033208. https://doi.org/10.1103/physreve.101.033208

Duan, D., He, J., Wu, H., & Verscharen, D. (2020). Magnetic energy transfer and distribution between protons and electrons for alfvénic waves at kinetic scales in wavenumber space. *The Astrophysical Journal*, *896*(1), 47. https://doi.org/10.3847/1538-4357/ab8ad2

Edyvean, J., Parashar, T. N., Simpson, T., Juno, J., Delzanno, G. L., Guo, F., et al. (2024). Scale separation effects on simulations of plasma turbulence. *The Astrophysical Journal*, *972*(2), 173. https://doi.org/10.3847/1538-4357/ad5cf5

Ergun, R., Goodrich, K., Wilder, F., Ahmadi, N., Holmes, J., Eriksson, S., et al. (2018). Magnetic reconnection, turbulence, and particle acceleration: Observations in the earth's magnetotail. *Geophysical Research Letters*, *45*(8), 3338–3347. https://doi.org/10.1002/2018gl076993

Fadanelli, S., Lavraud, B., Califano, F., Cozzani, G., Finelli, F., & Sisti, M. (2021). Energy conversions associated with magnetic reconnection. *Journal of Geophysical Research: Space Physics*, *126*(1), e2020JA028333. https://doi.org/10.1029/2020ja028333

Greco, A., Valentini, F., Servidio, S., & Matthaeus, W. H. (2012). Inhomogeneous kinetic effects related to intermittent magnetic discontinuities. *Physical Review E - Statistical Physics, Plasmas, Fluids, and Related Interdisciplinary Topics*, *86*(Part 2), 066405. https://doi.org/10.1103/PhysRevE.86.066405

Haggerty, C. C., Parashar, T. N., Matthaeus, W. H., Shay, M. A., Yang, Y., Wan, M., et al. (2017). Exploring the statistics of magnetic reconnection x-points in kinetic particle-in-cell turbulence. *Physics of Plasmas*, *24*(10), 102308. https://doi.org/10.1063/1.5001722

Hellinger, P., Montagud-Camps, V., Franci, L., Matteini, L., Papini, E., Verdini, A., & Landi, S. (2022). Ion-scale transition of plasma turbulence: Pressure–strain effect. *The Astrophysical Journal*, *930*(1), 48. https://doi.org/10.3847/1538-4357/ac5fad

Howes, G. G. (2008). Inertial range turbulence in kinetic plasmas. *Physics of Plasmas*, *15*(5), 055904. https://doi.org/10.1063/1.2889005

Jiang, K., Huang, S., Yuan, Z., Deng, X., Wei, Y., Xiong, Q., et al. (2021). Statistical properties of current, energy conversion, and electron acceleration in flux ropes in the terrestrial magnetotail. *Geophysical Research Letters*, *48*(11), e2021GL093458. https://doi.org/10.1029/2021gl093458

Karimabadi, H., Roytershteyn, V., Wan, M., Matthaeus, W. H., Daughton, W., Wu, P., et al. (2013). Coherent structures, intermittent turbulence, and dissipation in high-temperature plasmas. *Physics of Plasmas*, *20*(1), 012303. https://doi.org/10.1063/1.4773205

Lu, S., Angelopoulos, V., Artemyev, A., Pritchett, P., Liu, J., Runov, A., et al. (2019). Turbulence and particle acceleration in collisionless magnetic reconnection: Effects of temperature inhomogeneity across pre-reconnection current sheet. *The Astrophysical Journal*, *878*(2), 109. https://doi.org/10.3847/1538-4357/ab1f6b

Marshall, W. (1957). The kinetic theory of an ionized gas (part I) (Technical Report No. AERE-T/R-2247, pp. 21–27). United Kingdom Atomic Energy Authority. *Research Group. Atomic Energy Research Establishment, Harwell, Berks, England*. Retrieved from https://www.osti.gov/biblio/4141091

Matthaeus, W. H., Yang, Y., Wan, M., Parashar, T. N., Bandyopadhyay, R., Chasapis, A. r., et al. (2020). Pathways to dissipation in weakly collisional plasmas. *The Astrophysical Journal*, *891*(1), 101. https://doi.org/10.3847/1538-4357/ab6d6a

Parashar, T. N., & Matthaeus, W. H. (2016). Propinquity of current and vortex structures: Effects on collisionless plasma heating. *The Astrophysical Journal*, *832*(1), 57. https://doi.org/10.3847/0004-637X/832/1/57

Parashar, T. N., Shay, M. A., Cassak, P. A., & Matthaeus, W. H. (2009). Kinetic dissipation and anisotropic heating in a turbulent collisionless plasma. *Physics of Plasmas*, *16*(3), 032310. https://doi.org/10.1063/1.3094062

Pezzi, O., Liang, H., Juno, J., Cassak, P., Vásconez, C., & Sorriso-Valvo, L. (2020). Dissipation measures in weakly-collisional plasmas. *Monthly Notices of the Royal Astronomical Society*, *5*(5), 4857–4873.

Pezzi, O., Yang, Y., Valentini, F., Servidio, S., Chasapis, A., Matthaeus, W., & Veltri, P. (2019). Energy conversion in turbulent weakly collisional plasmas: Eulerian hybrid Vlasov–Maxwell simulations. *Physics of Plasmas*, *26*(7), 072301. https://doi.org/10.1063/1.5100125

Phan, T. D., Eastwood, J. P., Shay, M. A., Drake, J. F., Sonnerup, B. U. Ö., Fujimoto, M., et al. (2018). Electron magnetic reconnection without ion coupling in earth's turbulent magnetosheath. *Nature*, *557*(7704), 202–206. https://doi.org/10.1038/s41586-018-0091-5

Pongkitiwanichakul, P., Ruffolo, D., Guo, F., Du, S., Suetrong, P., Yannawa, C., et al. (2021). Role of parallel solenoidal electric field on energy conversion in 2.5 d decaying turbulence with a guide magnetic field. *The Astrophysical Journal*, *923*(2), 182. https://doi.org/10.3847/1538-4357/ac2f45

Ricci, P., Lapenta, G., & Brackbill, J. (2002). Gem reconnection challenge: Implicit kinetic simulations with the physical mass ratio. *Geophysical Research Letters*, *29*(23), 1–3. https://doi.org/10.1029/2002gl015314

Roy, S., Bandyopadhyay, R., Yang, Y., Parashar, T. N., Matthaeus, W. H., Adhikari, S., et al. (2022). Turbulent energy transfer and proton-electron heating in collisionless plasmas. *The Astrophysical Journal*, *941*(2), 137. https://doi.org/10.3847/1538-4357/aca479

Servidio, S., Matthaeus, W. H., Shay, M. A., Dmitruk, P., Cassak, P. A., & Wan, M. (2010). Statistics of magnetic reconnection in two-dimensional magnetohydrodynamic turbulence. *Physics of Plasmas*, *17*(3), 032315. https://doi.org/10.1063/1.3368798

Servidio, S., Valentini, F., Califano, F., & Veltri, P. (2012). Local kinetic effects in two-dimensional plasma turbulence. *Physical Review Letters*, *108*(4), 045001. https://doi.org/10.1103/PhysRevLett.108.045001

Sitnov, M., Merkin, V., Roytershteyn, V., & Swisdak, M. (2018). Kinetic dissipation around a dipolarization front. *Geophysical Research Letters*, *45*(10), 4639–4647. https://doi.org/10.1029/2018gl077874

Vörös, Z., Yordanova, E., Khotyaintsev, Y. V., Varsani, A., & Narita, Y. (2019). Energy conversion at kinetic scales in the turbulent magnetosheath. *Frontiers in Astronomy and Space Sciences*, *6*, 60. https://doi.org/10.3389/fspas.2019.00060

Wan, M., Matthaeus, W. H., Karimabadi, H., Roytershteyn, V., Shay, M., Wu, P., et al. (2012a). Intermittent dissipation at kinetic scales in collisionless plasma turbulence. *Physical Review Letters*, *109*(19), 195001. https://doi.org/10.1103/physrevlett.109.195001

Wan, M., Matthaeus, W. H., Karimabadi, H., Roytershteyn, V., Shay, M., Wu, P., et al. (2012b). Intermittent dissipation at kinetic scales in collisionless plasma turbulence. *Physical Review Letters*, *109*(19), 195001. https://doi.org/10.1103/PhysRevLett.109.195001

Wan, M., Matthaeus, W. H., Roytershteyn, V., Karimabadi, H., Parashar, T., Wu, P., & Shay, M. (2015). Intermittent dissipation and heating in 3d kinetic plasma turbulence. *Physical Review Letters*, *114*(17), 175002. https://doi.org/10.1103/physrevlett.114.175002

Wang, S., & Yang, Y. (2023). Electron heating associated with magnetic reconnection in foreshock waves: Particle-in-cell simulation analysis. *Journal of Geophysical Research*, *128*(11), e2023JA031672. https://doi.org/10.1029/2023ja031672

Wilder, F. D., Ergun, R. E., Eriksson, S., Phan, T. D., Burch, J. L., Ahmadi, N., et al. (2017). Multipoint measurements of the electron jet of symmetric magnetic reconnection with a moderate guide field. *Physical Review Letters*, *118*(26), 265101. https://doi.org/10.1103/PhysRevLett.118.265101

Wilder, F. D., Ergun, R. E., Burch, J. L., Ahmadi, N., Eriksson, S., Phan, T. D., et al. (2018). The role of the parallel electric field in electron-scale dissipation at reconnecting currents in the magnetosheath. *Journal of Geophysical Research*, *123*(8), 6533–6547. https://doi.org/10.1029/2018JA025529

Yang, Y. (2019). *Energy transfer and dissipation in plasma turbulence: From compressible mhd to collisionless plasma*. Springer.

Yang, Y., Matthaeus, W. H., Oughton, S., Bandyopadhyay, R., Pecora, F., Parashar, T. N., et al. (2024). Effective viscosity, resistivity, and Reynolds number in weakly collisional plasma turbulence. *Monthly Notices of the Royal Astronomical Society*, *528*(4), 6119–6128. https://doi.org/10.1093/mnras/stae355

Yang, Y., Matthaeus, W. H., Parashar, T. N., Haggerty, C. C., Roytershteyn, V., Daughton, W., et al. (2017a). Energy transfer, pressure tensor, and heating of kinetic plasma. *Physics of Plasmas*, *24*(7), 072306. https://doi.org/10.1063/1.4990421

Yang, Y., Matthaeus, W. H., Parashar, T. N., Wu, P., Wan, M., Shi, Y., et al. (2017b). Energy transfer channels and turbulence cascade in Vlasov-Maxwell turbulence. *Physical Review E - Statistical Physics, Plasmas, Fluids, and Related Interdisciplinary Topics*, *95*(6), 061201. https://doi.org/10.1103/PhysRevE.95.061201

Yang, Y., Matthaeus, W. H., Roy, S., Roytershteyn, V., Parashar, T. N., Bandyopadhyay, R., & Wan, M. (2022). Pressure–strain interaction as the energy dissipation estimate in collisionless plasma. *The Astrophysical Journal*, *929*(2), 142. https://doi.org/10.3847/1538-4357/ac5d3e

Yang, Y., Matthaeus, W. H., Shi, Y., Wan, M., & Chen, S. (2017c). Compressibility effect on coherent structures, energy transfer and scaling in magnetohydrodynamic turbulence. *Physics of Fluids*, *29*(3), 035105. https://doi.org/10.1063/1.4979068

Yang, Y., Pecora, F., Matthaeus, W. H., Roy, S., Cuesta, M. E., Chasapis, A., et al. (2023). Quantifying the agyrotropy of proton and electron heating in turbulent plasmas. *The Astrophysical Journal*, *944*(2), 148. https://doi.org/10.3847/1538-4357/acb25a

Yang, Y., Wan, M., Matthaeus, W. H., Sorriso-Valvo, L., Parashar, T. N., Lu, Q., et al. (2019). Scale dependence of energy transfer in turbulent plasma. *Monthly Notices of the Royal Astronomical Society*, *482*(4), 4933–4940. https://doi.org/10.1093/mnras/sty2977

Zeiler, A., Biskamp, D., Drake, J. F., Rogers, B. N., Shay, M. A., & Scholer, M. (2002). Three-dimensional particle simulations of collisionless magnetic reconnection. *Journal of Geophysical Research*, *107*(A9), 1230. https://doi.org/10.1029/2001JA000287

Zenitani, S., Hesse, M., Klimas, A., & Kuznetsova, M. (2011). New measure of the dissipation region in collisionless magnetic reconnection. *Physical Review Letters*, *106*(19), 195003. https://doi.org/10.1103/PhysRevLett.106.195003

Zhong, Z., Deng, X., Zhou, M., Ma, W., Tang, R., Khotyaintsev, Y. V., et al. (2019). Energy conversion and dissipation at dipolarization fronts: A statistical overview. *Geophysical Research Letters*, *46*(22), 12693–12701. https://doi.org/10.1029/2019gl085409